Multivariate analysis of the EW gauge bosons' polarisation at the LHC

Comité de Suivi Individuel

Mathis DUBAU
Laboratoire d'Annecy de Physique des Particules

20 June 2025

Standard Model

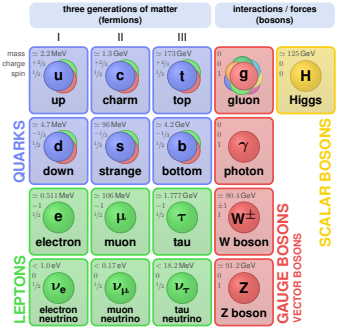

- Theory used in particle physics

- Highly accurate and extensively tested model

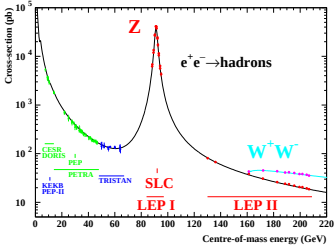

Cross section of $e^+e^- \rightarrow$ hadrons processes as a function of center-of-mass energy [1]

Invariant mass distribution of di-photon candidates for data at $\sqrt{s} = 13$ TeV [2]

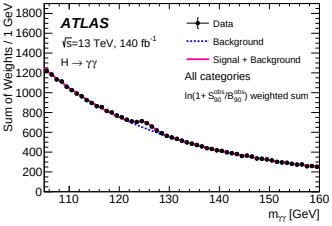

- Successfully confirmed by the discovery of the Higgs Boson in 2012 at the LHC by the ATLAS [3] and CMS [4] experiments

Tensions in the Standard Model

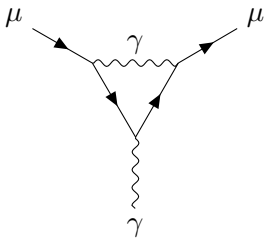

- 4.2σ deviation between the Fermilab measurement of the muon's magnetic moment [5] and the prediction by the *Muon g-2 Theory Initiative* [6]

- Lack of a dark matter candidate particle

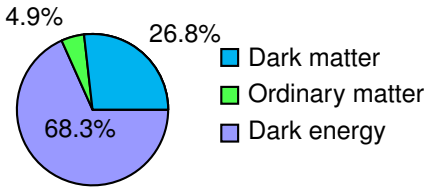

Energy density distribution of the Universe [7]

Plan

1. Vector Boson Scattering and Polarisation
2. e/γ
3. Scan of hyper-parameter space in BSM
4. Other works and Next steps

Spin

Intrinsic property of a particle

Massive vector bosons

3 degrees of freedom represented by 3 different polarizations, one arise from the Higgs mechanism when the bosons acquire mass

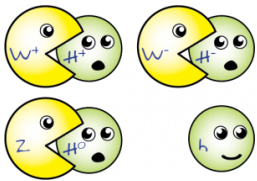

$$\epsilon_-^\mu = \frac{1}{\sqrt{2}}(0,1,-i,0) \quad \epsilon_0^\mu = \frac{1}{m_V}(k_z,0,0,E) \quad \epsilon_+^\mu = -\frac{1}{\sqrt{2}}(0,1,i,0)$$

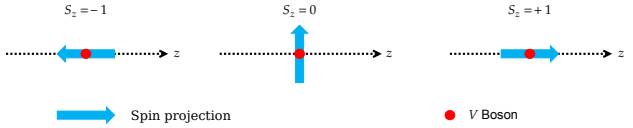

Representation of transverse (T or $\pm$) and longitudinal (0) polarisation states

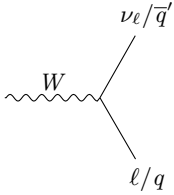

The decay products of W or Z bosons retain traces of the bosons' polarisation

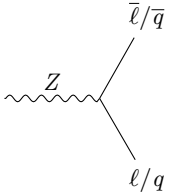

Why study Vector Boson Polarisation ?

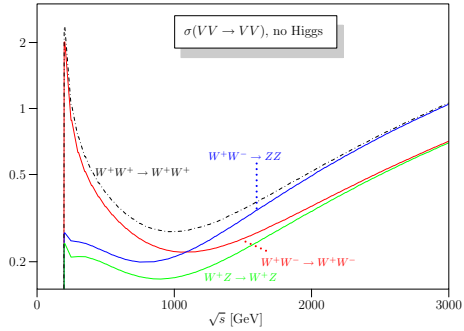

(a) Without Higgs boson

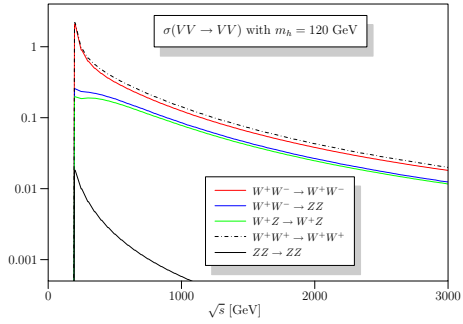

(b) With Higgs boson

Effective cross-section (in nb) for five different longitudinally polarized weak interaction gauge boson scattering (Vector Boson Scattering or VBS) processes [8]

Measuring polarisation in boson scattering (WZ production, for example) provides a direct probe of EW symmetry breaking mechanism

Standard Model cross section

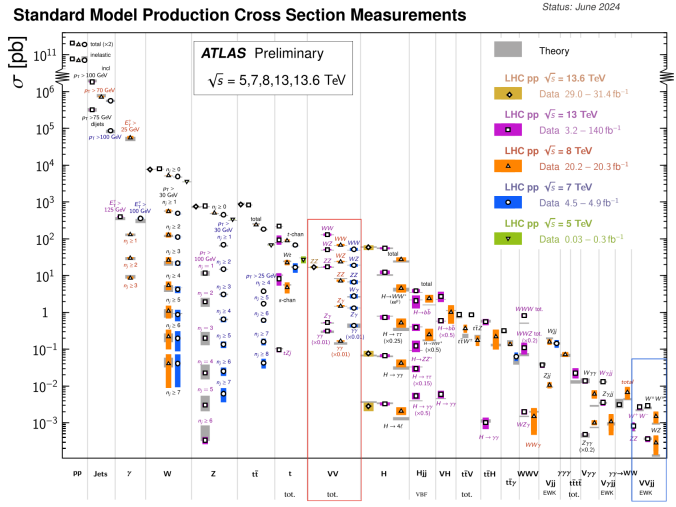

Summary of several Standard Model cross-section measurements [9]

My Analysis

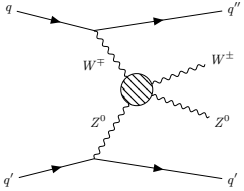

EWWZ VBS process

The ATLAS team at LAPP (Emmanuel, Iro, Lucia ...) has been analyzing WZ boson pairs for several years, in particular

- the first observation of the production of a WZ pair in an electroweak process [10]
- the first observation of the joint polarization states of gauge bosons in the WZ production [11]

- The main idea is to continue the previous work and try to measure now the fraction of polarisation in WZ VBS EW processes
- We focus on the WZjj$\rightarrow \ell\ell\ell\nu$jj decay channel with ℓ only e and μ
- Main challenge is the low cross section of this process

Analysis strategy

Work in parallel on two aspects

- Study machine learning techniques to maximize the sensitivity of WZjj-EW polarisation measurement $\longrightarrow$ done using existing published Run-2 WZ VBS analysis
- Develop analysis of Run-3 data for WZjj-EW measurement

Signal vs Background DNN

WZjj-EW vs Background → y axis

- 4 classes one-hot encoded → WZjj-EW, WZjj-QCD, ZZ-QCD, and other minor background, 1 for each process, 0 otherwise
- Softmax activation function for output
- ZZ-EW is not used for the training since it's signal-like
- output WZjj-EW used for y
- Weight event by event used, using the absolute value and matching N_{Signal} and $N_{\text{Background}}$

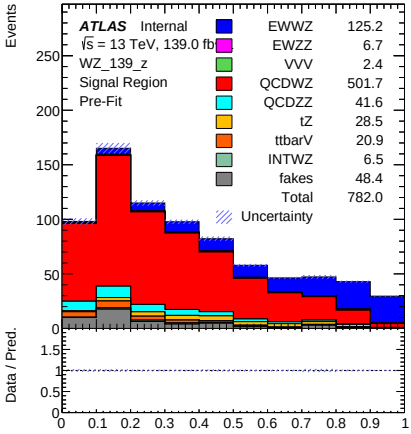

Signal vs Background template

Technical details on Backup Slides 3-4 and Variables in Table 1

Polarisation DNN - V1

- 4 output, one for each polarisation state
  - Weight event by event used, using the absolute value and matching $N_{\text{EW00/EW0T/EWT0}}$ and N_{EWTT}
- Softmax activation function for output

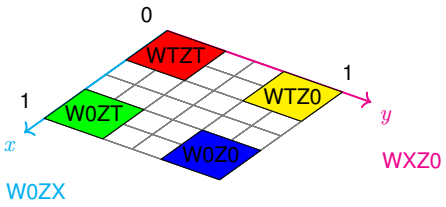

WXZ0

W0ZX

polarisation discrimination → (xy) plan

$$x = \frac{00 + 0T \times (1 - T0)}{00 + 0T + T0 + TT} \qquad y = \frac{00 + T0 \times (1 - 0T)}{00 + 0T + T0 + TT}$$

Technical details on Backup Slides 3-4 and Variables in Table 2

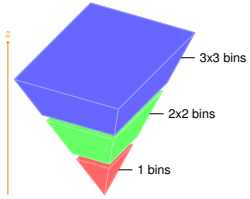

Custom binning in pyramidal shape

- 3 norm factor related to polarisation (despite other μ)
- more complex fit
- give a measurement on the 4 polarisation at the same time

Polarisation DNN - V2

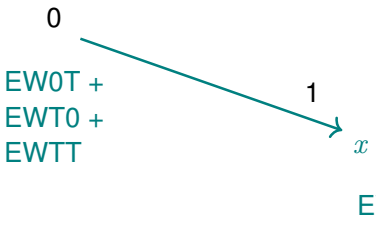

EW00 vs (EW0T+EWT0+EWTT) $\rightarrow$ x axis

- 1 single output $\rightarrow$ EW00 = 1 and EW0T+EWT0+EWTT = 0
- Sigmoid activation function for output
- Weight event by event used, using the absolute value and matching $N_{\text{EW00/EW0T/EWT0}}$ and N_{EWTT}

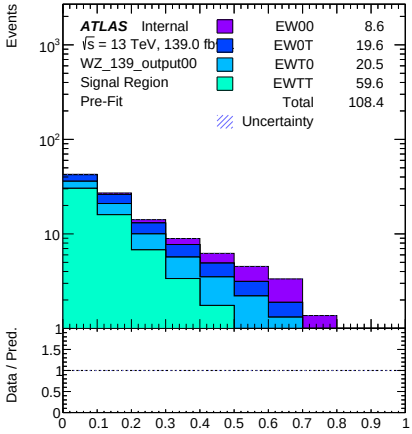

Polarisation template

Technical details on Backup Slides 3-4 and Variables in Table 2

k-fold

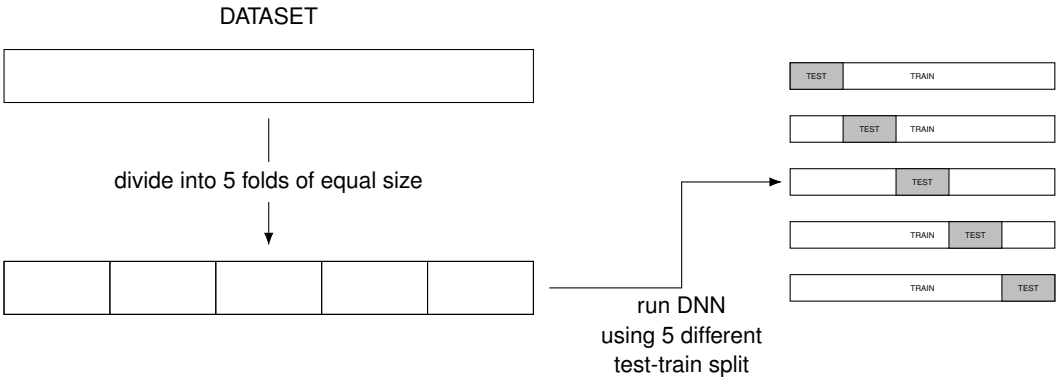

Implementation of a k-fold procedure $\longrightarrow$ suppression of any overfitting bias

$S/\sqrt{B}$ and K-Means

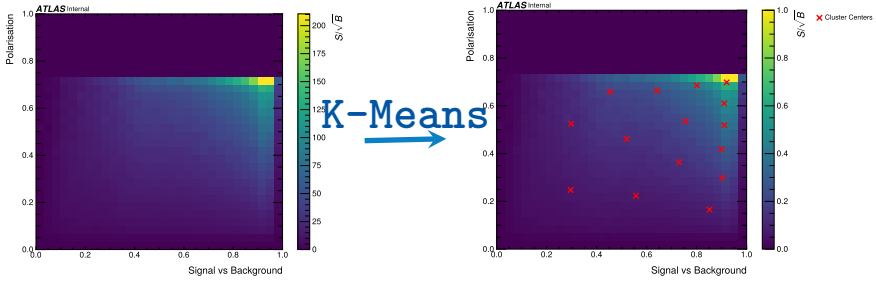

$S/\sqrt{B}$ 2D map

Voronoi Diagrams

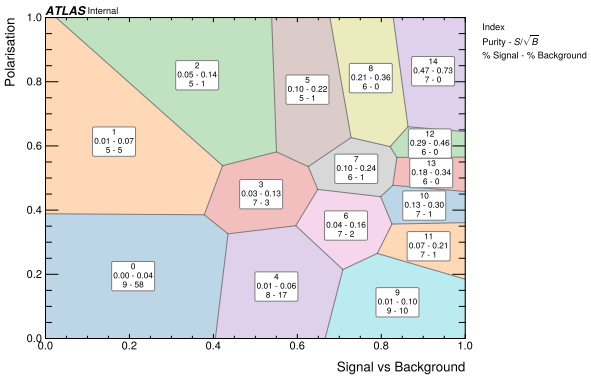

Voronoi Diagrams of our 2D map

- We construct a Voronoi Diagram using the function `Voronoi` from SciPy
- The seeds are the clusters centres computed before
- For each Voronoi region we present:
  - the index $\longrightarrow$ the bin number when moving to 1D
  - the purity, $S/(S+B)$, with weight
  - the ratio $S/\sqrt{B}$, with weight
  - the $\%$ of Signal and Background, with weight

2D Fit - Joint Polarisation

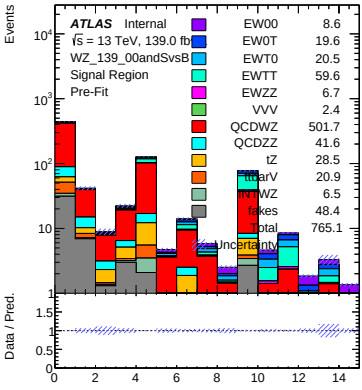

2D unrolled template for EW00

Fit details on Backup Slides 7, 9, 10

Type	Date	Bins	Significance		
			Run-2	Run-3	Run-2+3
3D map - first stage of the fit	10/2024	27	0.54	0.88	1.30
3D map - actual fit setup	02/2025	27	0.54	0.80	0.97
3D map - binning optimisation	04/2025	14	0.60	0.89	1.07
2D map - multi-output polarisation	06/2025	14	0.69	1.03	1.24
2D map - single-output polarisation	06/2025	15	0.91	1.33	1.59

- Constant optimisation and improvement $\longrightarrow$ improvement of the significance
- Over 160% improvement since the first fit
- Non linear binning optimisation is functional

2D Fit - Single Polarisation

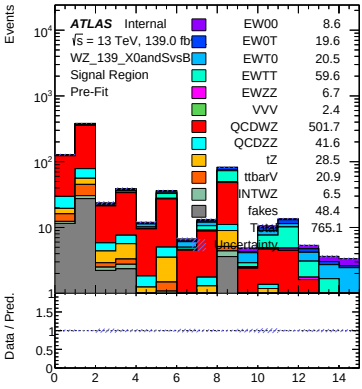

2D unrolled template for EWX0

Fit details on Backup Slides 7, 8, 10

Type	Bins	Significance		
		Run-2	Run-3	Run-2+3
2D map - EW0X	15	1.84	2.68	3.20
2D map - EWX0	15	2.28	3.33	4.0

- More than 3σ for Run-2+3
- Non linear binning optimisation is functional

Forward electrons ID

Improved $|\eta|$ coverage rate from 2.5 to 4.0 during ATLAS Phase-II Upgrade, enabling more "forward" e/μ to be used

- QT: based on the Forward electron ID in Run-4 with ITk and HGTD with definition of working point
- An issue in p_{T} calibration was observed and we proposed a DNN for calibrating it (only in Run-4)
- Portage of the ID technique to Run-3 and proposition of working point

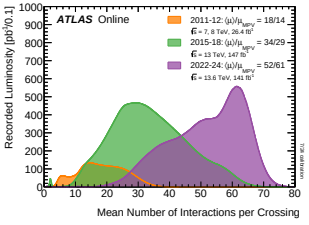

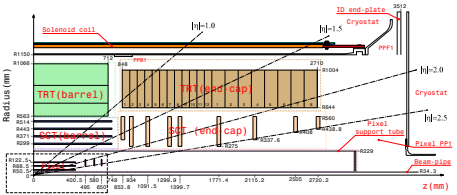

Current Trajectograph [12]

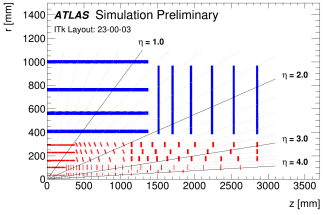

Inner Tracker (ITk) [13]

Methodology

- Trying to set up a discriminant:
  - with variables uncorrelated to p_{T}
  - trained over all p_{T}

In order to:

- Be able to measure a distortion of shape from a unique DNN in order to compute selection efficiency for all p_{T} in a correlated way (hope is that, as the discriminant is less p_{T}-dependent, the mis-modeling would also be much less p_{T} dependent)
- Allow extrapolation at high-p_{T} for working point

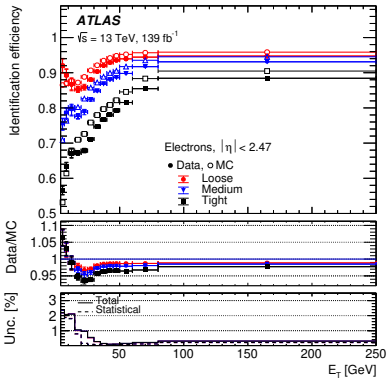

Identification efficiencies of electrons from $Z \longrightarrow ee$ decays as a function of the electron's E_{T} [14]

Run-4 - Calibration

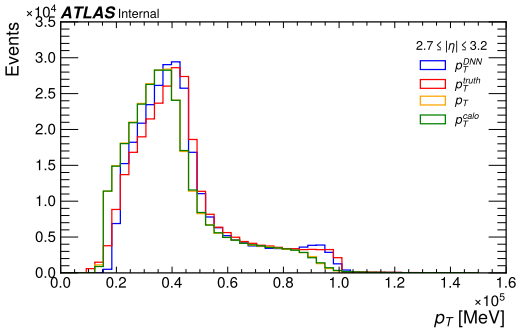

p_{T} from different methods

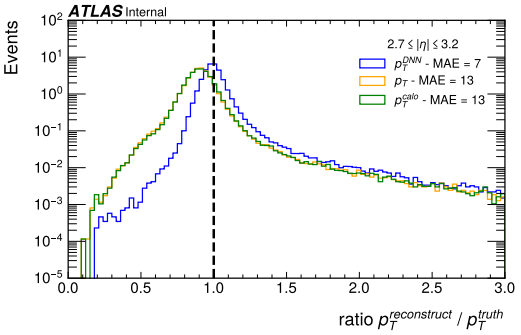

Ratio between p_T^{truth} and $p_T^{\mathrm{reconstruct}}$

$$MAE = \frac{\sum_{i=1}^{N} |y_i - s(x_i)|}{N}$$

- y_i the label $\longrightarrow$ p_T^{truth}
- x_i is the vector of input variables
- $s(x_i)$ the prediction made by the DNN $\longrightarrow$ p_T^{DNN}

Decorrelation

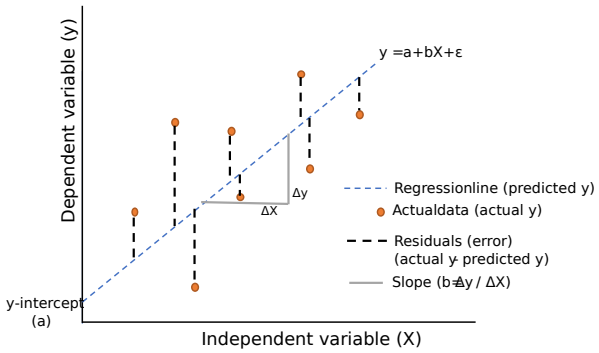

Linear regression and residuals

- Decorrelation between p_T^{calo} for Run-3 and p_T^{DNN} for Run-4 and the seven clusters moments
- Training a linear regression model to fit p_{T} versus the 7 C.M (for signal only)
- We take the residuals to subtract them to the C.M (background and signal)
- The p_{T} variable is then unchanged, and is uncorrelated from the 7 C.M

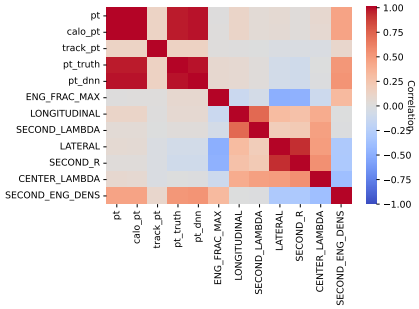

Before uncorrelation

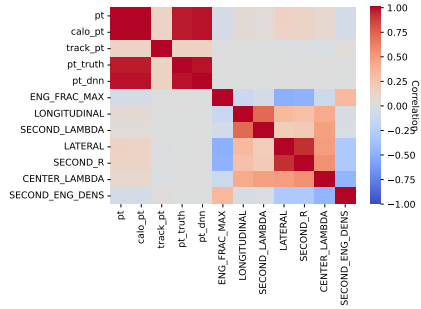

After uncorrelation

Correlation matrix between p_{T} and the seven clusters moments for the signal before and after uncorrelated them with a linear regression model
example for Run-4 with $2.7 \leq |\eta| \leq 3.2$ and $\langle \mu \rangle = 200$

As expected, the decorrelation process allows for using in the DNN these 7 input variables independent of pT

WP cuts

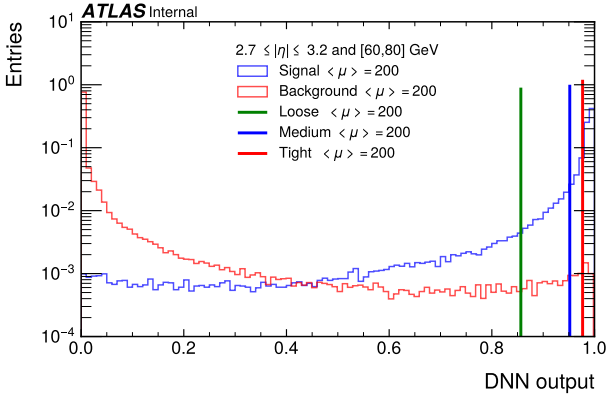

DNN prediction for signal and background at $\langle\mu\rangle = 200$ with cut on signal efficiency
example for $2.7 \leq |\eta| \leq 3.2$ and $p_T \in [60; 80]$ GeV

Variables in Table 3

- Cut on the DNN predictions for the signal at $\langle\mu\rangle = 200$ for Run-4 and $\langle\mu\rangle \in [40; 60]$ for Run-3
- Background is not take into acount on the cut
- loose WP as 90% signal efficiency
- medium WP as 80% signal efficiency
- tight WP as 70% signal efficiency

Run-4 - DNN WP Signal efficiency

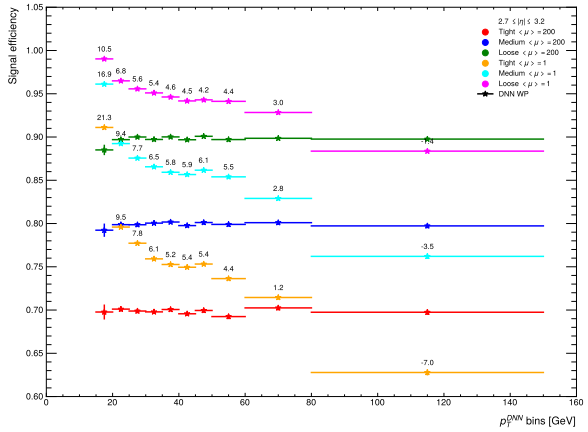

Signal efficiency for DNN WP for data test at $\langle\mu\rangle = 200$ and $\langle\mu\rangle = 1$

- Signal efficiency at $\langle\mu\rangle = 1$ is a few percent higher than $\langle\mu\rangle = 200$ for loose and medium
- The sensitivity of the signal selection to pile-up is only a few percent
- No interpolation possible $\longrightarrow$ missing samples at different $\langle\mu\rangle$

Run-3 - DNN Loose WP Signal efficiency

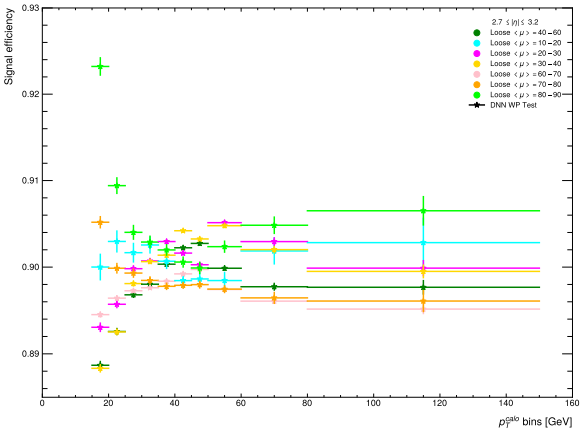

Signal efficiency for the Loose DNN working points on the test dataset at every $\langle \mu \rangle$ bins

- Overall the interpolation on the pile-up is working well and allow us to bring back the working points efficiencies within $\sim$ 1% of the desired values.

Results for Medium and Tight WP on Backup slide 13 and 14

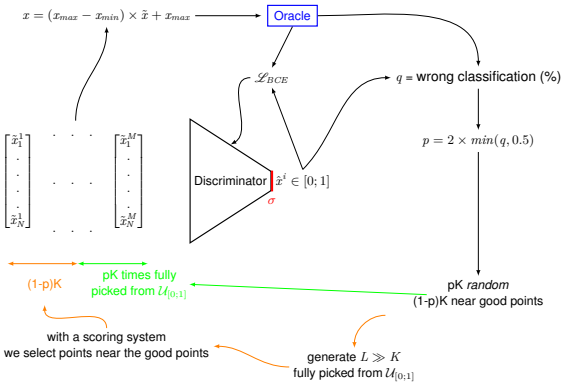

Schema of AL using DNN

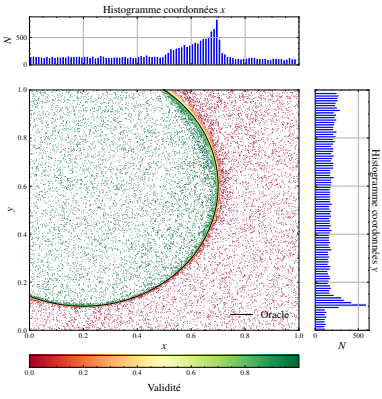

Toy model with the DNN and the AL algorithm

- Scoring methods based on [15]
- Collaboration with Ugo de Noyers and Björn Herrmann from LAPTh

- Scan of Scotogenic Models [16] using MCMC
- Paper to be published and Ugo's PhD Thesis

1. Vector Boson Scattering and Polarisation
2. e/γ
3. Scan of hyper-parameter space in BSM
4. Other works and Next steps

Other works

ADUM hours

- Research ethics - 15h
- Researh integrity - 15h
- Fundamentals of Big Data - 24h
- Gif School 2023 - 24h
- PhD and career development - 24h
- Introduction to parallel computing - 36h
- European School of High Energy Physics - 40h
- Teach TD efficiently - 7h
- 21h30 of lectures on Introduction to python for 1st year student at the USMB

Talks

- COPIN-IN2P3 - Talk in Cracaw on WZ inclusive polarisation studies [11]
- e/γ workshop 2025
- Physics ATLAS France (PAF)

Extra Work

- Qualified ATLAS author
- Vulgarisation scientifique pour Fête de la science of LAPP 2023 and at Mercredi du LAPP
- CERN Guide
- Shift in the control room for the Calorimeter / Forward detector desk - 208h
- Develop a website to visualise our datasets
- e/γ workshop 2024

Next Steps

e/γ

- Implementation of the DNN for Identification and Calibration inside ATLAS `Athena` Framework

The analysis

- Update (reconstructed) object systematics for Run-3 data
- Study of associated systematic uncertainties through the statistical treatment
- Follow the ATLAS procedures in order to eventually uncover the data and get the physics results

Work on the side

- Finish paper publication with Ugo and Björn
- Write the thesis

Summary

VBS and Polarisation

- DNN optimisation is done $\longrightarrow$ gain of significance
- k-fold and binning optimisation is showing good results
- Implementation done in the framework
- The fit setup is done, we need to add the systematics now
- Best significance ever presented with more than 1.5σ for joint polarisation and more than 3σ for single polarisation for Run-2+3
- Joint and Single Boson polarisation measurement

e/γ

- Calibration of the p_{T} work well and give us a more precise value rather than the existing methods
- DNN WP outperform the pre-existing WP
- WP efficiency works well at different $\langle\mu\rangle$ and the interpolation if successfully by giving us overall $\sim$ 1% difference in signal efficiencies

BSM

- New methods to scan an hyper-parameter space
- Show good results and comparison with MCMC
- Paper soon to published

References

[1] *Precision electroweak measurements on the Z resonance*, Phys. Rept. **427** (2006) 257, arXiv: hep-ex/0509008 (Cited on slide 2).

[2] ATLAS Collaboration, *Measurement of the Higgs boson mass with $H \longrightarrow \gamma\gamma$ decays in 140 fb1 of $\sqrt{s} = 13$ TeV pp collisions with the ATLAS detector*, Physics Letters B **847** (2023) 138315, URL: http://dx.doi.org/10.1016/j.physletb.2023.138315 (Cited on slide 2).

[3] *Observation of a new particle in the search for the Standard Model Higgs boson with the ATLAS detector at the LHC*, Physics Letters B **716** (2012) 1, URL: https://doi.org/10.1016/j.physletb.2012.08.020 (Cited on slide 2).

[4] *Observation of a new boson at a mass of 125 GeV with the CMS experiment at the LHC*, Physics Letters B **716** (2012) 30, URL: https://doi.org/10.1016/j.physletb.2012.08.021 (Cited on slide 2).

[5] B. Abi et al., *Measurement of the Positive Muon Anomalous Magnetic Moment to 0.46 ppm*, Phys. Rev. Lett. **126** (2021) 141801, arXiv: 2104.03281 [hep-ex] (Cited on slides 3, 40).

[6] T. Aoyama et al., *The anomalous magnetic moment of the muon in the Standard Model*, Phys. Rept. **887** (2020) 1, arXiv: 2006.04822 [hep-ph] (Cited on slides 3, 40).

[7] G. Hinshaw et al., *Nine-Year Wilkinson Microwave Anisotropy Probe (WMAP) Observations: Cosmological Parameter Results*, Astrophys. J. Suppl. **208** (2013) 19, arXiv: 1212.5226 [astro-ph.CO] (Cited on slide 3).

[8] Ana Alboteanu, Wolfgang Kilian, and Jürgen Reuter, *Resonances and unitarity in weak boson scattering at the LHC*, Journal of High Energy Physics **2008** (2008) 010 (Cited on slide 8).

[9] *Standard Model Summary Plots June 2024*, (2024) (Cited on slide 9).

[10] ATLAS Collaboration, *Observation of electroweak $W^{\pm}Z$ boson pair production in association with two jets in pp collisions at $\sqrt{s} = 13$ TeV with the ATLAS detector*, Physics Letters B **793** (2019) 469 (Cited on slide 10).

[11] ATLAS Collaboration, *Observation of gauge boson joint-polarisation states in $W^{\pm}Z$ production from pp collisions at $\sqrt{s} = 13$ TeV with the ATLAS detector*, 2022, arXiv: 2211.09435 [hep-ex] (Cited on slides 10, 32).

[12] *The ATLAS Experiment at the CERN Large Hadron Collider*, JINST **3** (2008) S08003, Also published by CERN Geneva in 2010,
URL: https://cds.cern.ch/record/1129811 (Cited on slide 21).

[13] *Expected tracking and related performance with the updated ATLAS Inner Tracker layout at the High-Luminosity LHC*, tech. rep., All figures including auxiliary figures are available at https://atlas.web.cern.ch/Atlas/GROUPS/PHYSICS/PUBNOTES/ATL-PHYS-PUB-2021-024: CERN, 2021,
URL: https://cds.cern.ch/record/2776651 (Cited on slide 21).

[14] *Electron and photon efficiencies in LHC Run 2 with the ATLAS experiment*, Journal of High Energy Physics **2024** (2024),
URL: http://dx.doi.org/10.1007/JHEP05(2024)162 (Cited on slide 22).

[15] Mark D. Goodsell and Ari Joury, *Active learning BSM parameter spaces*, Eur. Phys. J. C **83** (2023) 268, arXiv: 2204.13950 [hep-ph] (Cited on slide 30).

[16] Ugo de Noyers, Maud Sarazin, and Björn Herrmann, *Phenomenology of a singlet-doublet-triplet scotogenic framework*, (2024), arXiv: 2410.23712 [hep-ph] (Cited on slide 30).

[17] Louis Portales, *Observation of electroweak WZjj production and studies on pile-up mitigation with the ATLAS detector*, Theses: Université Savoie Mont Blanc, 2020,
URL: https://theses.hal.science/tel-03550156 (Cited on slide 47).

[18] Martín Abadi et al., *TensorFlow: Large-Scale Machine Learning on Heterogeneous Systems*, Software available from tensorflow.org, 2015,
URL: https://www.tensorflow.org/ (Cited on slide 44).

[19] François Chollet et al., *Keras*, `https://keras.io`, 2015 (Cited on slide 44).

5 Backup slides

- Framework
- DNN configuration
- Fit details
- e/γ

Muon g-2

The Dirac equation predict $g = 2$
In nature, radiate corrections make $g \neq 2$

We can compute a the anomaly:

$$a = \frac{g-2}{2}$$

with g the Landé factor that arise from:

$$\vec{\mu}_S = g\frac{q}{2m}\vec{S}$$

The values observed for now are the following:

- $a_\mu(\text{Exp}) = 116592061(41) \times 10^{11}$[5]
- $a_\mu(\text{SM}) = 116591810(43) \times 10^{11}$[6]

Analysis set-up, phase space and events selection

- Exactly same event selection as used for Run-2 (inclusive and VBS), see below
- CP recommendations and ID/ISO WP points adapted to Run-3
- lepton / boson / jet information

Phase space definition

Variables	Fiducial WZjj-EW
Lepton $\|\eta\|$	< 2.5
p_T of l_Z, p_T of l_W [GeV]	$> 15, > 20$
m_Z range [GeV]	$\left\|m_Z - m_Z^{PDG}\right\| < 10$
m_T^W [GeV]	≥ 30
$\Delta R(l_Z^-, l_Z+), \Delta R(l_Z, l_W)$	$> 0.2, > 0.3$
p_T two leading jets [GeV]	> 40
$\|\eta_j\|$ two leading jets	< 4.5
Jets multiplicity	≥ 2
$\eta_{j1} \cdot \eta_{j2}$	< 0
m_{jj} [GeV]	> 500
$\Delta R(j, l)$	> 0.3
$N_{b-quark}$	$= 0$

Event selection

Parameter	Criteria
ZZ veto	Less than 4 baseline leptons
N leptons	Exactly 3 leptons passing the Z selection
Leading lepton p_T	$p_T^{\text{lead}} > 25$ GeV in 2015 and $p_T^{\text{lead}} > 27$ GeV in 2016-2018
Z leptons	Two same flavor oppositely charged leptons passing Z-lepton selection
Mass window	$\|m_{\ell\ell} - m_Z\| < 10$ GeV
W lepton	Remaining lepton passes W lepton selection
W transverse mass	$m_T^W > 30$ GeV
Jet multiplicity	≥ 2
p_T of two tagging jets	> 40 GeV
$\|\eta\|$ of two tagging jets	> 4.5
η of two tagging jets	opposite sign
m_{jj}	> 150 GeV

- ZZ CR: $\geq$4 baseline leptons
- b CR: $N_{b-quark} > 0$
- WZjj-QCD VR: $m_{jj} < 500$ GeV

Setup

We use `Tensorflow` [18] and his API `Keras` [19] to compute deep neural networks
The dataset, signal + background, is normalised for better performance with following normalization:

$$x_{norm} = \frac{x - x_{max}}{x_{max} - x_{min}}$$

to scale them between 0 and 1
For multiple output DNN, we one-hot encoded each output as 1 for the corresponding process and 0 otherwise. We use in this way the categorical cross entropy function:

$$\mathscr{L} = \frac{-1}{N} \sum_{i=1}^{N} \sum_{c=1}^{C} x_{i,c} \cdot \ln\left(\hat{x}_{i,c}\right)$$

For multiple output DNN, we use the binary cross-entropy loss function:

$$\mathscr{L} = \frac{-1}{N} \sum_{i=1}^{N} \left[(1 - y_i) \ln\left(1 - s(x_i)\right) + y_i \ln s(x_i)\right]$$

We split the dataset as 80% of it for training and 20% for validation following a k-fold procedure

Neural Network Architecture

Feed-Forward fully connected DNN

- number of hidden layers 6 each of them with ReLU activation function
- number of neuron per hidden layers 256
- a dropout layer after each hidden layer with a dropout of 0.25 except the last layer
- output layer with:
  - one single output with Sigmoid activation function
  - multiple output with Softmax activation function

The training was then done with the following settings:

- The optimizer for the loss function is `Adam` with an initial learning rate of 10^{-3} and a weight decay of 0.5
- We use a learning rate scheduler to decrease it by a facotr by 0.33 value when `val_loss` don't improve for 5 epochs and with a lower limit at 10^{-10}
- The input layer is made of N_{input} neurons
- We use an early stopper to prevent overfitting with a patience of 10 epochs
- Batch size of 10240

Activation Function

$$ReLU(x) = \begin{cases} x & \text{if } x > 0 \\ 0 & \text{else} \end{cases}$$

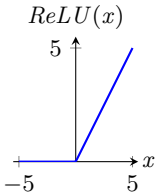

ReLU (*Rectified Linear Unit*) function

$$\sigma(x) = \frac{1}{1 + \exp^{-x}}$$

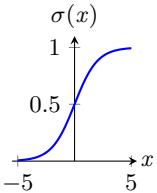

Sigmoid function

$$\sigma(x_i) = \frac{e^{x_i}}{\sum_{j=1}^{C} e^{x_j}}$$

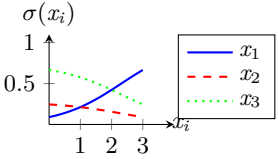

Softmax function for three input values (x_1, $x_2 = 1$, $x_3 = 2$)

Variables

Table 1: Signal vs Background DNN variables

Symbol	Description
N^{jets}	Multiplicity of jets
m_{jj}	Mass of the di-jet system
$\Delta\eta_{jj}$	Difference in pseudorapidity between the two tagging jets
$\Delta\phi_{jj}$	Difference in azimuth angle between the two tagging jets
p_T^W	Transverse impulse of the W
$p_T^{\text{jet-1}}$	Transverse impulse of the tagging jet 1
$\eta^{\text{jet-2}}$	Pseudorapidity of the tagging jet 2
ζ_{lep}	Centrality of leptons with respect to the di-jet system
$\lvert y_W - y_Z \rvert$	Difference in rapidity between Z boson and lepton from W
$\cos\theta_V$	Cosine of emission angle in the WZ rest frames
$R_{p_T}^{\text{hard}}$	Transverse component of vector sum of moments divided by their p_T sum
η_{W_l,Z_l}	Pseudorapidity of the first leptons from W and Z
p_T^{WZ}	Transverse impulse of the WZ system
$\Delta\phi(l_1^Z, l_2^Z)$	Difference of azimuthal angle ϕ of leptons from Z
$\Delta\phi(l^W, l^\nu)$	Difference in azimuthal angle ϕ of leptons from W
$E^{\text{jet-1}}$	Energy of of the tagging jet 1
$A_{p_T^{jj}}$	Asymmetry between the p_T of the two tagging jets

Variables from BDT [17]

Table 2: Polarisation DNN variables

Symbol	Description
$\Delta\eta_{jj}$	Difference in pseudorapidity between the two tagging jets
$\Delta\phi_{jj}$	Difference in azimuth angle between the two tagging jets
$p_T^{W,Z}$	Transverse impulse of the W and Z bosons
$\eta^{\text{jet-1/2}}$	Pseudorapidity of the tagging jet 1 and 2
ΔR_{jZ}	Angular separation between the first tagging jet and the Z boson
m_T^{WZ}	Transverse mass of system WZ
$\lvert y_W - y_Z \rvert$	Difference in rapidity between Z boson and lepton from W
$\cos\theta_{W,Z,V}$	Cosine of emission angle in the W, Z, and WZ rest frames
$p_T^{Z_1}$	Transverse impulse of the first lepton from Z
η_{W_l,Z_l}	Pseudorapidity of the three leptons from W and Z
p_T^{WZ}	Transverse impulse of the WZ system
$\Delta\phi(l_1^Z, l_2^Z)$	Difference of azimuthal angle ϕ of leptons from Z
$A_{p_T^{jj}}$	Asymmetry between the p_T of the two tagging jets
r^{21}	Ratio of p_T of leading to sub-leading boson

Samples of the fit

Signal

- VBS WZjj-EW
  - SR: 4 polarised "new" with a rescaling to match previous samples number of events
  - bCR and ZZCR: unpolarised "noSkim"

Background

- VBS WZjj-EW off-shell
  - SR: unpolarised "noSkim" rescale to HT/2 and substract by unpolarised "new" $\longrightarrow$ not implemented due to yields issues on "new" polarised samples
- VBS WZjj-EW interference between polarisation states
  - SR: unpolarised "new" substract by 4 polarised "new" $\longrightarrow$ not implemented due to yields issues on "new" polarised samples
- ZZ-EW, VVV, WZjj-QCD, ZZ-QCD, tZ, $t\bar{t}V$, WZ-INT
  - SR
  - bCR and ZZCR
- Fakes - $t\bar{t}$, $Z\gamma$, $Z\ell\ell$
  - SR: rescaling of 1.8 for the MC estimate to match the numbers of events expected by the Matrix Method
  - bCR: Matrix Method estimate
  - ZZCR: MC estimate since low in this region

Single Boson polarisation

POI: $N_{\text{EW}}^{\text{observed}}$, f_1

$$\frac{N_{\text{EW}}^{\text{observed}}}{N_{\text{0X/X0}}^{\text{predict}}} * f_1$$
$$\frac{N_{\text{EW}}^{\text{observed}}}{N_{\text{TX/XT}}^{\text{predict}}} * (1 - f_1)$$

Parameters that are floating unconstrained in the fit, others ones are constant

f_1 is set to be f_{0X}/f_{X0} so $f_{00} + f_{0T}/f_{00} + f_{T0}$

The first norm factor is applied to EW0X/EWX0 while the second to EWTX/EWXT

Joint Boson polarisation

POI: $N_{\text{EW}}^{\text{observed}}$, f_1

$$\frac{N_{\text{EW}}^{\text{observed}}}{N_{00}^{\text{predict}}} * f_1$$
$$\frac{N_{\text{EW}}^{\text{observed}}}{N_{0T+T0+TT}^{\text{predict}}} * (1 - f_1)$$

Parameters that are floating unconstrained in the fit, other ones are constant

f_1 is set to be f_{00}

The first norm factor is applied to EW00 while the second to EW0T, EWT0 and EWTT

Parameters of the fit

NormFactor

A floating norm factor μ if given for (as from previous analysis):

- $t\bar{t}V$
- tZ
- WZjj-QCD
- ZZ-QCD only for ZZCR

Fit

The fit is done using a SR and two control region:

- SR: unrolled 3D map from the DNN
- ZZCR: m_{JJ}
- bCR: BDT_b

all are compute directly from the output of the framework

Hybrid-Asimov fit (only CR have data unblinded)

Higher significance is done using a `Lumi`

5 Backup slides

- Framework
- DNN configuration
- Fit details
- e/γ

Variables

Detector	Variables names	Variables information
HGTD	Time	HGTD time information
Calorimeter	η^{calo}	η from `CaloCluster`
	ϕ^{calo}	ϕ from `CaloCluster`
	f_i^{EM}	Deposit energy on the i-th layer of the EMCalo for $i \in [1;2;3]$
	f_i^{HAD}	Deposit energy on the i-th layer of the HADCalo for $i \in [1;2;3;4]$
	f_{fem}	Fraction of the cluster energy that is deposited in the most energetic cell of the cluster
	longitudinal	Shower shape in the clusters' longitudinal direction, based on the distance of each cell to the shower core
	$< \lambda^2 >$	Second moment in λ - the distance of each cell to the cluster center along the shower axis
	lateral	Lateral moment of the shower taking into account the two most energetic cells (which constitutes the shower core)
	$< r^2 >$	Second moment in r - the radial distance of each cell to the shower axis
	λ_{center}	The distance of the shower center from the front of the calorimeter along the shower axis
	$< \rho^2 >$	Second moment in energy density
Tracker	η^{track}	η from `trackParticle`
	ϕ^{track}	ϕ from `trackParticle`
	pixels	Number of pixels hits
	strips	Number of strips hits
Track-Calo match	$\Delta\eta$	Delta in η for the point of impact of the trace in layer 2 of the calo and the energy deposit in this same layer
	$\Delta\eta$	Delta in ϕ for the point of impact of the trace in layer 2 of the calo and the energy deposit in this same layer
	$\Delta\eta^{\text{rescaled}}$	Delta in ϕ for the point of impact of the trace rescaled by the energy give by the calorimeter
	$\Delta\eta^{\text{last}}$	

Table 3: Variables used as input for Run-4 and Run-3

Six first Cluster Moments (f_{fem}, `longitudinal`, $< \lambda^2 >$, `lateral`, $< r^2 >$ and λ_{center}) are the ones to ID the electron in the forward region presently

Variables examples

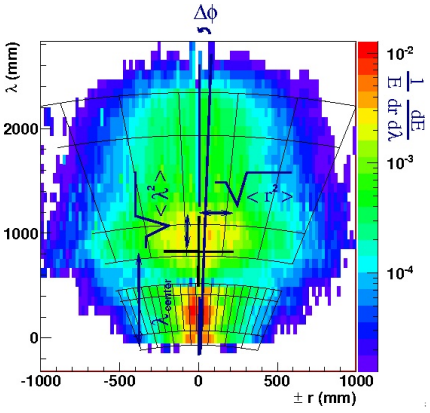

Clusters moments varaibles

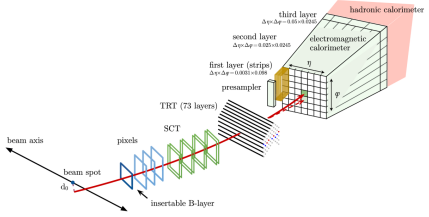

Current Trajectograph

Example of variables we can get from the detectors

Run-3 - DNN Medium WP Signal efficiency - $\langle\mu\rangle$ interpolation

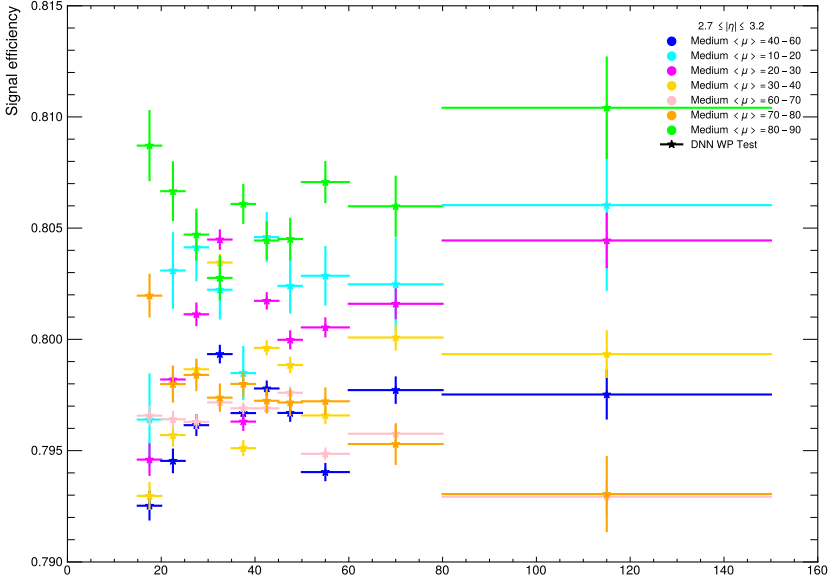

Run-3 - DNN Tight WP Signal efficiency - $\langle\mu\rangle$ interpolation